PNNL-24362

Pacific Northwest
NATIONAL LABORATORY
Proudly Operated by Battelle Since 1965

# Rolling Process Modeling Report: Finite-Element Model Validation and Parametric Study on Various Rolling Process Parameters

**June 2015**

A Soulami
CA Lavender
DM Paxton
DE Burkes

U.S. DEPARTMENT OF ENERGY

Prepared for the U.S. Department of Energy
under Contract DE-AC05-76RL01830

PACIFIC NORTHWEST NATIONAL LABORATORY
*operated by*
BATTELLE
*for the*
UNITED STATES DEPARTMENT OF ENERGY
*under Contract DE-AC05-76RL01830*

**Printed in the United States of America**

**Available to DOE and DOE contractors from the**
**Office of Scientific and Technical Information,**
**P.O. Box 62, Oak Ridge, TN 37831-0062;**
**ph: (865) 576-8401**
**fax: (865) 576-5728**
**email: reports@adonis.osti.gov**

**Available to the public from the National Technical Information Service**
**5301 Shawnee Rd., Alexandria, VA 22312**
**ph: (800) 553-NTIS (6847)**
**email: orders@ntis.gov <http://www.ntis.gov/about/form.aspx>**
**Online ordering: http://www.ntis.gov**


This document was printed on recycled paper.
(8/2010)

PNNL-24362

# Rolling Process Modeling Report: Finite-Element Model Validation and Parametric Study on Various Rolling Process Parameters

A Soulami
CA Lavender
DM Paxton
DE Burkes

June 2015

Prepared for
the U.S. Department of Energy
under Contract DE-AC05-76RL01830

Pacific Northwest National Laboratory
Richland, Washington 99352

# Abstract

Pacific Northwest National Laboratory (PNNL) has been investigating manufacturing processes for the uranium-10% molybdenum alloy plate-type fuel for high-performance research reactors in the United States. This work supports the U.S. Department of Energy National Nuclear Security Administration's Office of Material Management and Minimization Reactor Conversion Program. This report documents modeling results of PNNL's efforts to perform finite-element simulations to predict roll-separating forces for various rolling mill geometries for PNNL, Babcock & Wilcox Co., Y-12 National Security Complex, Los Alamos National Laboratory, and Idaho National Laboratory. The model developed and presented in a previous report has been subjected to further validation study using new sets of experimental data generated from a rolling mill at PNNL. Simulation results of both hot rolling and cold rolling of uranium-10% molybdenum coupons have been compared with experimental results. The model was used to predict roll-separating forces at different temperatures and reductions for five rolling mills within the National Nuclear Security Administration Fuel Fabrication Capability project. This report also presents initial results of a finite-element model microstructure-based approach to study the surface roughness at the interface between zirconium and uranium-10% molybdenum.

# Acronyms and Abbreviations

| | |
|---|---|
| B&W | Babcock and Wilcox |
| FEM | finite-element model |
| FFC | Fuel Fabrication Capability |
| INL | Idaho National Laboratory |
| LANL | Los Alamos National Laboratory |
| PNNL | Pacific Northwest National Laboratory |
| RVE | representative volume element |
| U-10Mo | uranium-10 wt% molybdenum |

# Contents

# Figures



# Tables

# 1.0 Introduction

The transition from high-enriched uranium fuel to low-enriched uranium fuel in research and test reactors has been a global focus for the past three decades (Snelgrove et al. 1997). The U.S. Department of Energy National Nuclear Security Administration's Office of Material Management and Minimization Reactor Conversion Program is currently considering uranium alloyed with nominally ten weight percent Mo (referred to as U-10Mo) as a monolithic low-enriched uranium fuel with the potential to replace highly enriched uranium fuel in nuclear research and test reactors. In U-10Mo, the molybdenum in the alloy stabilizes the cubic gamma phase, allowing for acceptable swelling behavior under irradiation (Lee et al. 1997, Park et al. 2001, Meyer et al. 2002, Ozaltun et al. 2011). A monolithic U-10Mo foil encapsulated in aluminum alloy cladding possesses the greatest possible low-enriched uranium density in the fuel region, maintains excellent resistance to anisotropic growth (i.e., swelling), and is compatible with existing reactor designs. In addition, the U-10Mo fuel alloy represents a good combination of irradiation performance, oxidation resistance, strength, and ductility. Therefore, it is ideal for reducing nuclear proliferation risks associated with the transportation and storage of large quantities of high-enriched uranium.

Extensive research has been conducted regarding process-variable relationships during hot rolling and methods to predict changes in resultant sheet metal characteristics. However, the majority of this research has focused on conventional structural metals (e.g., steel) and little has focused on development of predictive tools that can be applied to hot rolling of uranium alloys in the form of bare or encapsulated coupons. When designing hot-rolling schedules, the ability to quickly investigate the influence of process variables on properties (e.g., roll-separation force) and possible defects (e.g., thickness uniformity, dog-boning, and waviness) is highly desirable. Understanding these properties and possible defects is important for optimizing process efficiency, achieving desired foil quality, engineering desired foil characteristics, and developing reasonable production schedules on a rational scientific basis.

A finite-element model (FEM) of the pack-rolling process of U-10Mo canned in AISI 1018 steel was previously developed (Soulami et al. 2014) and shown to correlate well to experimental roll-separation forces and pack thicknesses observed in actual rolling operations at INL. This model was used to explain dog-boning defects attributed to a mismatch in flow stress of the 1018 steel and the U-10Mo at the ends of the roll pack. Using a can material with a flow stress that more closely matches that of U-10Mo would likely reduce or eliminate dog-boning. Waviness, another common defect that occurs during rolling, was also predicted by the model and was observed to be more pronounced in the case of rolling inside a 1018 steel can when compared to rolling with a 304 stainless steel can or a Zircaloy-2 (Zr-2) can. Bare-rolling case simulations predicted an almost perfect foil with no waviness. Overall, model predictions indicated that reducing the mismatch in strength between the can material and the fuel core would lead to fewer defects.

The goal of the process modeling effort is to provide members of the Fuel Fabrication Capability (FFC) project that are rolling uranium-10 wt% molybdenum (U-10Mo) with the data needed to be sure they are rolling a high quality product in the most efficient manner possible. Therefore, the effort has focused on validation of the models with actual rolling data from Pacific Northwest National Laboratory (PNNL) and Idaho National Laboratory (INL) rolling mills. Through verification and validation, the model was used to determine forces at various rolling mills under many temperatures, reductions per pass, and input/output thicknesses. As a result, Babcock & Wilcox Co. (B&W) has successfully rolled U-

10Mo at approximately 600°C using 40% reduction of area rather than the small conservative reductions (typically less than 10%) previously used for U-10Mo. The model predicted that the rolling forces would be within the capability of the B&W mill and was further validated by the successful demonstration.

An additional validation study of the model that investigates the mechanical behavior of U-10Mo coupons during cold- and hot-rolling processes is reported. Simulated roll-separating forces are compared to actual measurements from PNNL's rolling mill. This validation study also allowed for calibration of the friction parameter for contact between the rolls and rolled coupons. In addition, the model was used to perform a parametric study on the effect of roll diameter and temperature on the roll-separating force. The results of this study are intended to afford other rolling mill operators within the FFC project an approximation of separating forces they may encounter for a given rolling schedule, i.e., reduction and temperature. Finally, this report presents preliminary results of the microstructure-based FEM investigating the surface roughness at the interface between Zr and U-10Mo. The results presented in this report can assist FFC partners in optimizing the parameters governing the thermomechanical processing and fabrication of U-Mo fuel foils.

# 2.0 FEM Validation through Comparison with PNNL Measurements

The FEM of the rolling process was validated in a previous report using a comparison between simulations and measured data from actual rolling experiments conducted at INL (Soulami et al. 2014). Simulations were conducted following a schedule used at INL and using U-10Mo mechanical properties obtained from compression tests performed at PNNL and reported in Joshi et al. (2013). These simulations consisted of hot rolling the roll packs. These roll packs consisted of an inner picture-frame piece and top and bottom cover plates (see Figure 1). The thickness of the frame was sized to the approximate thickness of the U-10Mo alloy coupon. Physical dimensions of the roll pack were set to match the size of the U-10Mo coupon. Coupons simulated for this study were the size used to produce a mini foil. Mini-foil alloy coupon dimensions are nominally 1.16" long × 0.73" wide × 0.107" thick. The outer dimensions of the roll-pack frame are nominally 0.75" greater in both length and width than those of the coupon. The cover plates are nominally 0.13" thick.

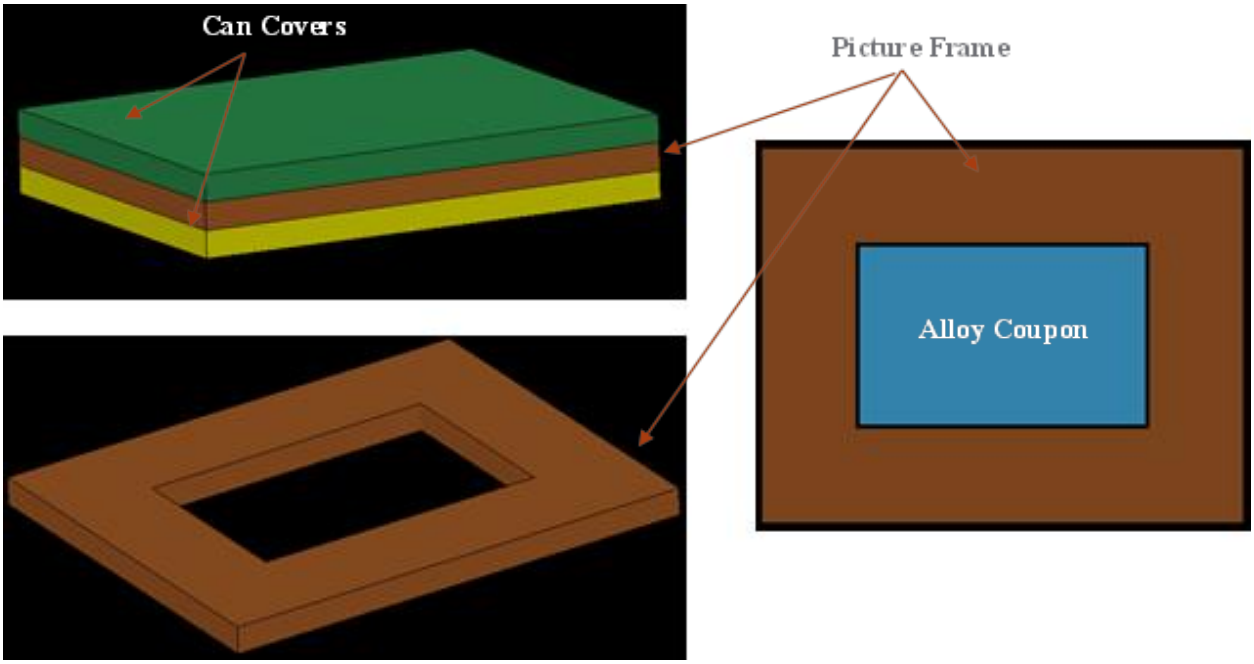


**Figure 1**. Representation of the Full Roll Pack. The blue area represents the alloy coupon, the green area is the top cover of the can, the yellow area is the bottom cover of the can, and the brown area is the frame.

Figure 2 shows both the PNNL compression data and a comparison between measured roll-separating force and roll-separating force simulated using properties from the literature (Sim using literature data) and from PNNL compression tests (Sim using pnnl compression data). For better agreement with the measured values, the Sim using pnnl compression data roll-separating force took into account material work hardening for temperatures below 550°C (1020°F). When using PNNL compression data, the shift to the top of the roll-separating force curve after introducing the work hardening, as noted by compression tests, can clearly be observed. Note that the simulated roll-separating forces using PNNL compression data deviate less than 3% from the measured data over the entire rolling schedule, whereas the simulated roll-separating forces using literature data deviate approximately 7%.

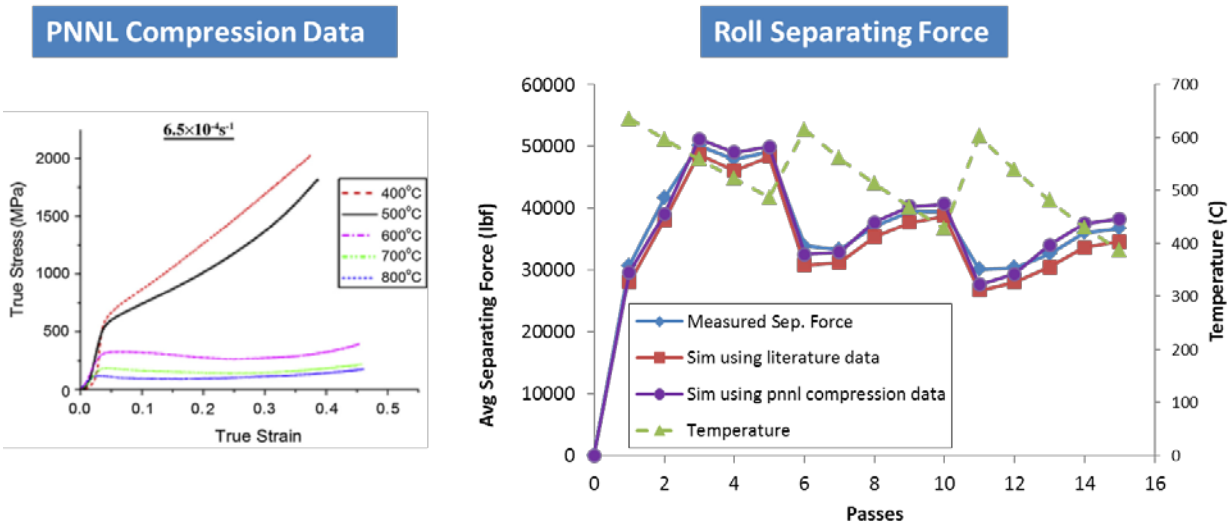


**Figure 2**. Stress-Strain Curve from PNNL Compression Data (left); Measured Roll-Separating Forces Compared to Simulated Roll-Separating Forces (using mechanical properties from the literature and PNNL compression tests) (right)

Friction between the rolls and the rolled specimen is an important factor affecting the accuracy of the predicted roll-separating forces. In fact, several processing parameters such as reduction, rolling speed, rolling temperature, and surface roughness affect the friction coefficient. Since accurate measurement of friction coefficients is very challenging, a range of values 0.3 to 0.6 were obtained from inverse calculations matching the predicted load-separating force with the measurements using PNNL's rolling mill. Because the PNNL rolling mill is equipped with a load cell, it can accurately measure roll-separating forces during the rolling process. Sun et al. (2005) studied the effect of hot-rolling process parameters on friction for 1018 stainless steel. They back-calculated the friction coefficient using a numerical model, validated through comparison with experimental measurements, that relates the friction coefficient to rolling temperature, rolling speed, and reduction. They estimated the friction coefficient to be ~0.26 for a rolling temperature of 850°C. Similar values were also reported in Lenard et al. (1999). Table 1 compares PNNL rolling mill measurements and FEM simulations for a 15% reduction at 700°C (1290°F) with those for a 10% cold reduction.

**Table 1**. Simulated and Measured (using PNNL 4" diameter rolling mill) Roll-Separating Forces at 700°C (1290°F)

| Reduction (%) | Thickness (in.) | | | Measured Mill Load (lbf) | Simulated Mill Load, F (lbf) |
|---|---|---|---|---|---|
| | Desired | Actual | Simulated | | |
| 15 | 0.125 | 0.123 | 0.126 | 21,952 | Fric 0.3 → F = 20,488<br>Fric 0.5 → F = 22,913 |
| 10 | 0.129 | 0.133 | 0.131 | 31,068 | Fric 0.3 → F = 29,752<br>Fric 0.5 → F = 33,094 |

Simulated roll-separating forces and coupon thicknesses are in good agreement with the measured roll-separating forces and coupon thicknesses for friction coefficients in the range of 0.3 to 0.5. For ensuing calculations, a friction coefficient of 0.3 was used based on better agreement with the experimental results reported in Table 1. Figure 3 plots the roll-separation forces for nine passes at 700°C

(1290°F). Each pass represents a 15% reduction rate. Simulated results are consistent with measured results using a friction coefficient of 0.3. The PNNL results, along with the INL results presented in detail in the previous modeling report (Soulami et al. 2014), further validate the FEM. The PNNL results provide added confidence in the ability of the model to accurately predict roll-separating forces.

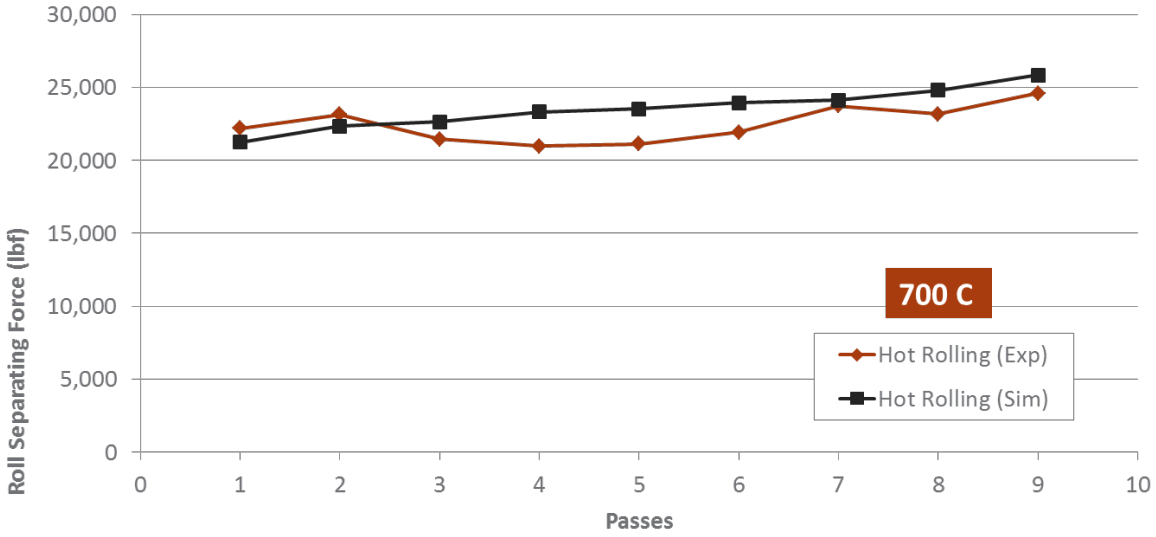


**Figure 3**. Comparison between Simulated and Measured Results Using the PNNL Rolling Mill at 700°C (1290°F) Maximum Deviation is ~12.5%.

# 3.0 Parametric Study

## 3.1 Effect of Roll Diameter and Temperature for the Five FFC Project Rolling Mills

The FEM was used to conduct a parametric study on the influence of roll diameter, temperature, reduction, and sample width on the roll-separating force and strain. Table 2 summarizes the roll diameters of the five FFC project rolling mills. Table 3 presents roll-pack dimensions analyzed using half symmetry for length and width, and full thickness.

**Table 2**. Roll Diameter for Hot Rolling for the Five FFC Project Rolling Mills

| PNNL | Los Alamos National Laboratory (LANL) | INL | Y-12 Nuclear Security Complex | B&W |
|---|---|---|---|---|
| 4" | 8" | 10" | 13" | 16" |

**Table 3**. Roll-Pack Dimensions

| Coupon (U-10Mo) | | | Can Assembly (AISI 1018) | | | | Roll Pack |
|---|---|---|---|---|---|---|---|
| Length | Width | Thickness | Length | Width | Frame Thickness | Cover Thickness | Thickness |
| 3.315" | 2.635" | 0.141" | 4.3" | 4.3" | 0.141" | 0.125" | 0.407" |

### 3.1.1 Roll-Separating Forces

The simulated roll-separating forces for the five FFC project rolling mills are shown as a function of the reduction at 800°C (1470°F) in Figure 4 and at 600°C (1110°F) in Figure 5 for the roll-pack dimensions provided in Table 3. Use of larger roll diameters clearly requires the mill to accommodate greater separating forces, especially at lower temperatures as a result of increased contact area between the roll-pack and roll face and high reduction rates because of an increase in flow stress. Roll separating force also becomes somewhat non-linear at higher reduction rates with increased roll diameter also as a result of the increased contact area and flow stress (work hardening) under these conditions.

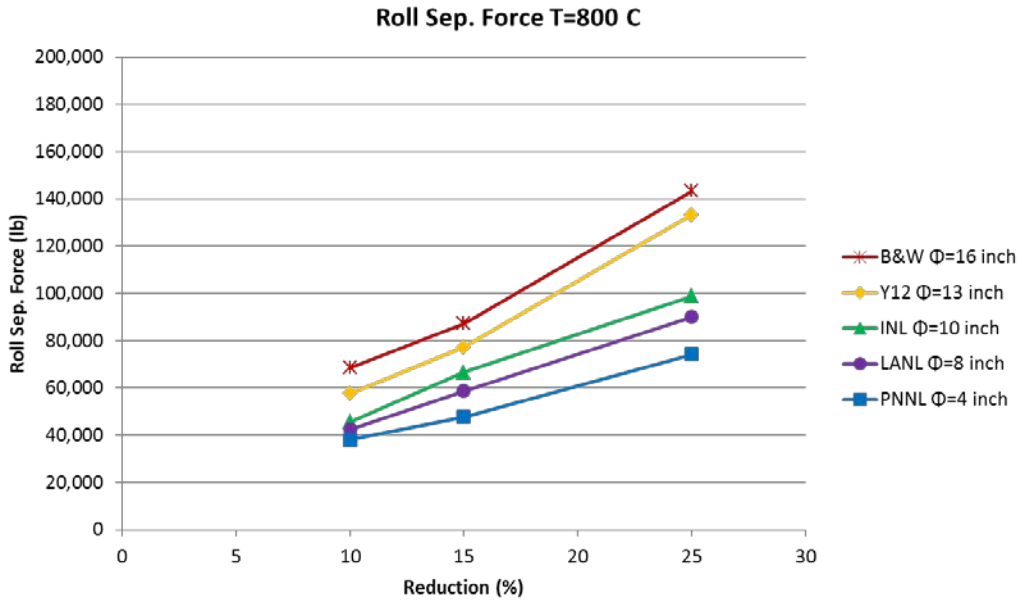


**Figure 4**. Roll-Separating Forces at Various Reductions for the Five FFC Project Rolling Mills at 800°C (1470°F)

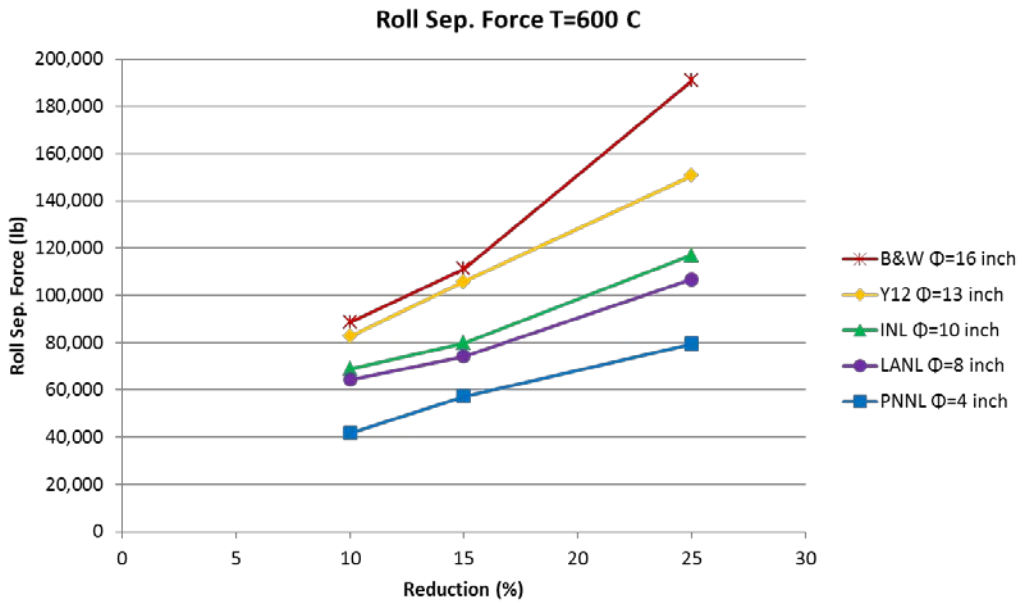


**Figure 5**. Roll-Separating Forces at Various Reductions for the Five FFC Project Rolling Mills at 600°C (1110°F)

### 3.1.2 Strain

The effective plastic strain at the center of the U-10Mo coupon as function of the roll diameter is shown for different reductions at 800°C (1470°F) in Figure 6 and at 600°C (1110°F) in Figure 7.

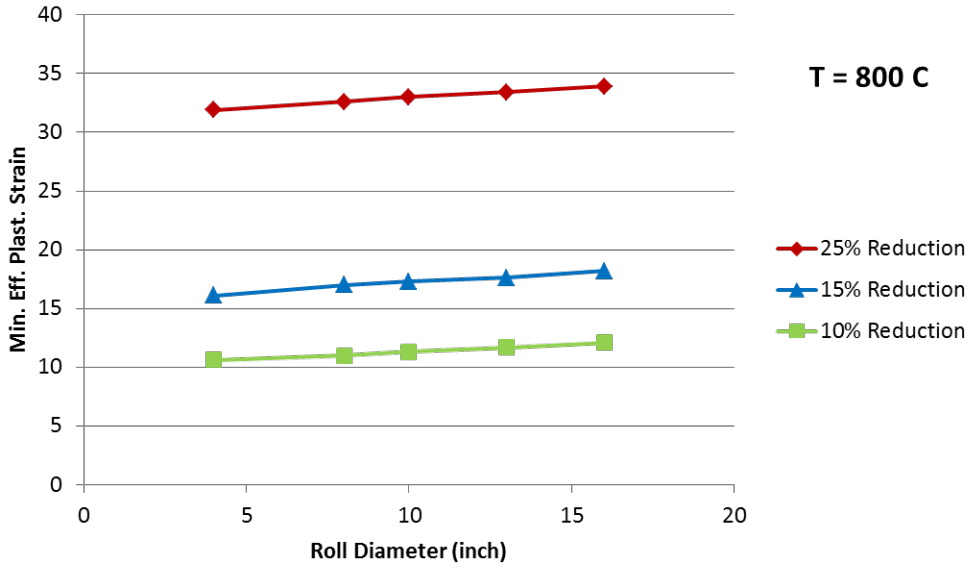


**Figure 6**. Effective Plastic Strain as a Function of Roll Diameter at Various Reductions at 800°C (1470°F)

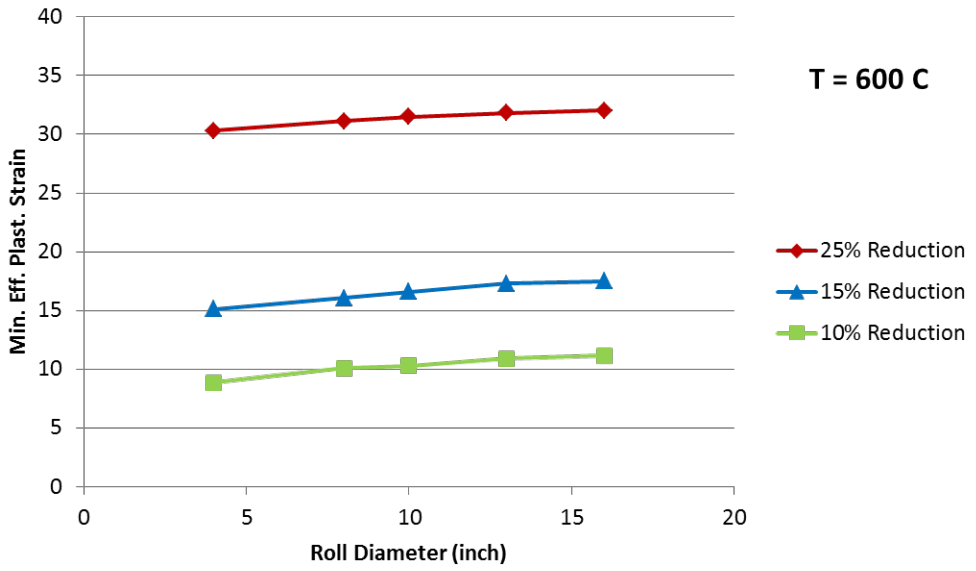


**Figure 7**. Effective Plastic Strain as a Function of Roll Diameter at Various Reductions at 600°C (1110°F)

These results again indicate that roll-separating force increases with roll diameter and reduction rate and decreases at higher temperatures. An increase of approximately 3% can be observed in the strain going from small to large roll diameters. In addition, effective plastic strain is close to the reduction rate at 10% and 15%, but higher at 25%. Note that effective plastic strain contains contributions from longitudinal, transverse, and through-thickness strains; therefore, those values are expected to be higher than the reduction rate. Larger-diameter rolls apply more deformation on a larger zone below the contact area than smaller rolls do.

Another important aspect is the reduction. Small reductions cause deformation only near the surface of the coupons and almost no deformation at the center. To illustrate this phenomenon, Figure 8 shows thickness strain contours for the LANL rolling mill at 15% and 25% reductions and Figure 9 shows thickness strain contours for the B&W rolling mill at a 1.5% reduction. The contrast is apparent between a uniform strain distribution at higher reductions and only surface deformation with no plastic deformation at the center of the coupon at lower reductions.

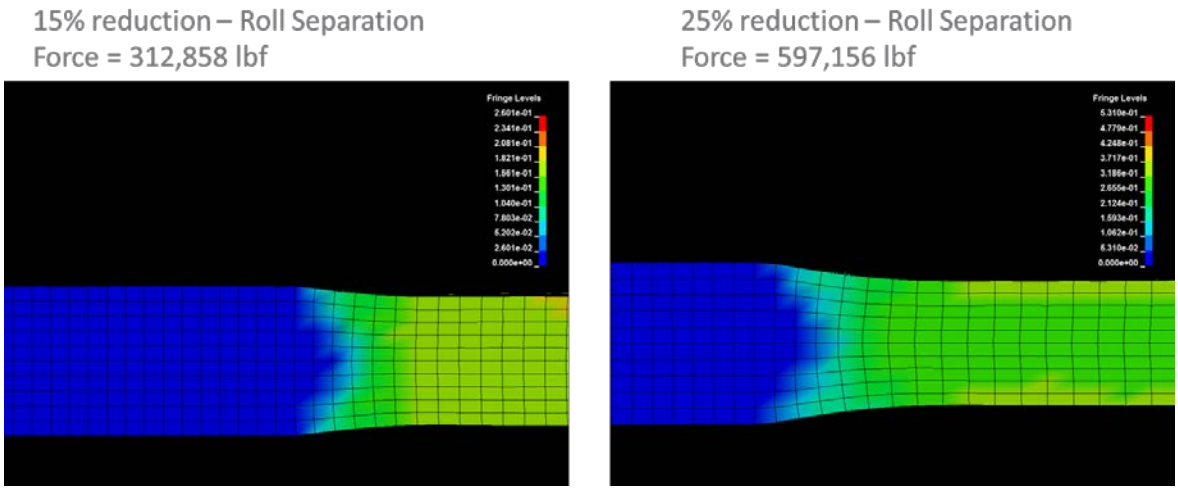


**Figure 8**. Through-Thickness Strain Contours for LANL Mill at 15% and 25% Reductions

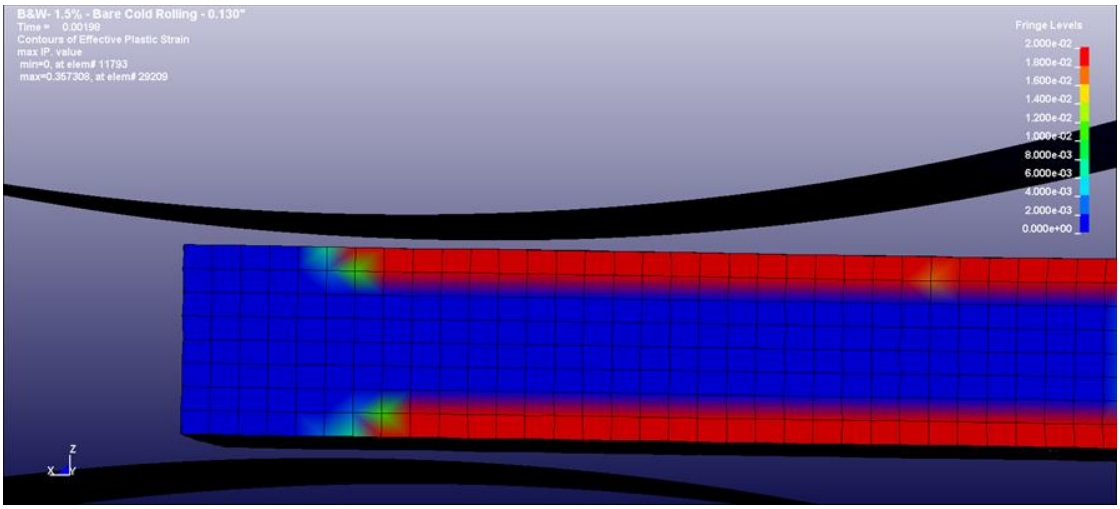


**Figure 9**. Through-Thickness Strain Contours for B&W Mill at 1.5% Reduction

## 3.2 B&W Process Parameters

This section presents additional simulation results using B&W rolling mill geometry. Cold-rolling simulations were conducted using the FEM and various results were extracted (i.e., roll-separating forces and mill stiffness as function of coupon width, thickness, and friction).

Figure 10 plots roll-separating force and rolling mill stiffness as a function of the coupon thickness, with 0.200" being the thickest coupon that the FFC intends to roll at this time. While a friction coefficient of 0.3 was assumed for these simulations, it should be noted that a higher friction coefficient would increase roll-separating force and rolling mill stiffness further (as demonstrated in Table 1). This is especially important if the goal is to reduce the number of passes and thus increase both reduction rates and the initial thickness of the coupons. However, the B&W hot and cold rolling mills possess adequate stiffness and roll separating force capacity to accommodate friction coefficients beyond 0.5 (results of which are not presented here). The results clearly show that while use of thinner coupons / ingots

requires less roll separating force, a significantly higher roll mill stiffness is required. Use of thicker coupons / ingots require a less stiff mill, but higher roll separating force capability is necessary.

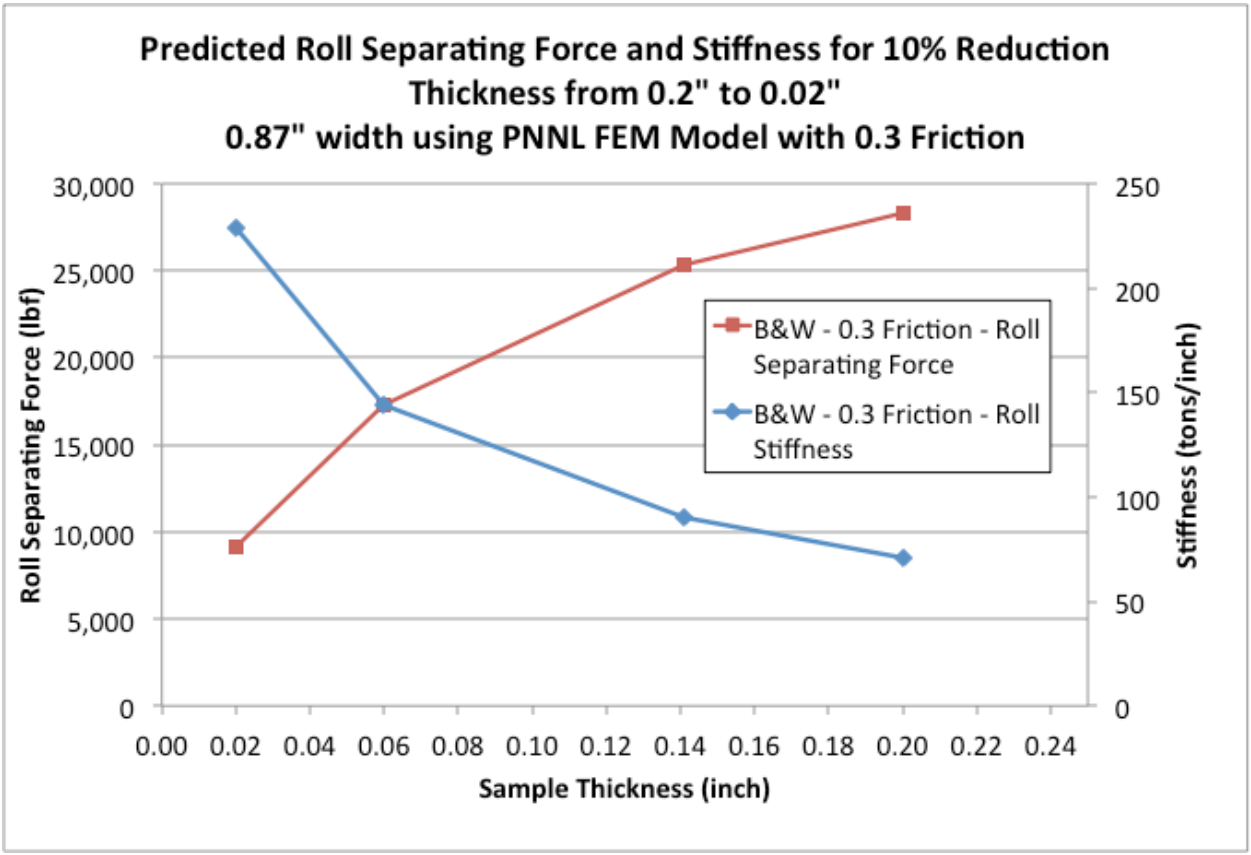


**Figure 10**. Roll-Separating Force and Roll Mill Stiffness as a Function of Samples Thickness for the B&W Mill with a 16" Roll Diameter and Friction Coefficient of 0.3

Cold-rolling simulations using the B&W rolling mill (roll diameter of 3.75") were also conducted on samples with different widths ranging from 0.875" to 5", with 5" representing the widest coupon that the FFC intends to roll at this time, as a function of different initial sample thickness. Roll separating force simulations are plotted in Figure 11 using a 0.3 friction coefficient and a 10% reduction. The equivalent rolling mill stiffness for the same simulations is provided in Figure 12. The roll-separating force and rolling mill stiffness clearly increased with sample width, while as shown previously, roll-separating force increased with increasing sample thickness while roll stiffness decreased with increasing sample thickness. These results can be used as guidance on sample design, knowing the rolling mill separating force maximum capacity, which is approximately 300 tons for the B&W cold rolling mill. Thus, the B&W cold rolling mill should be able to easily accommodate the sample dimensions currently being targeted by the FFC.

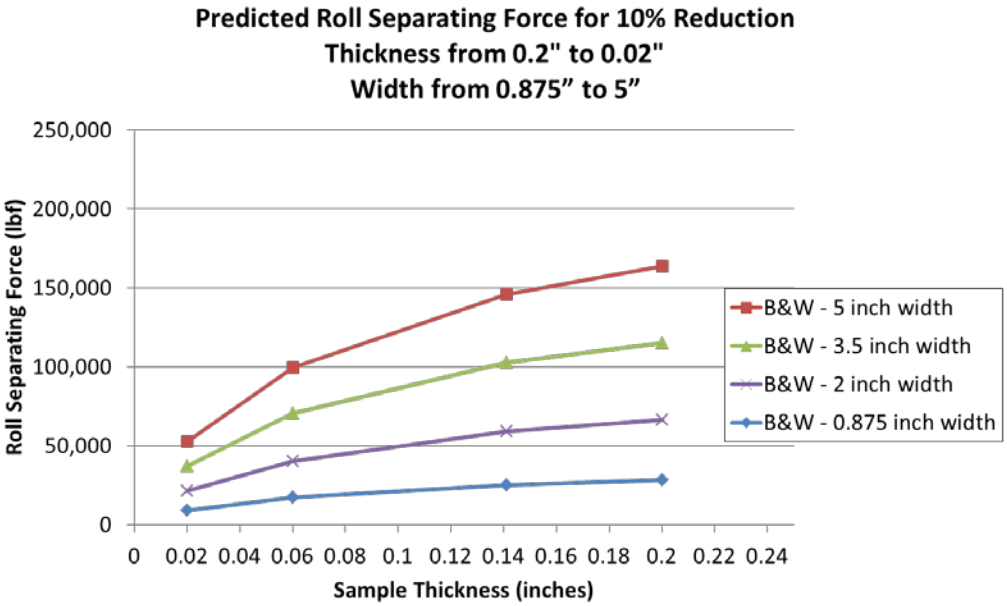


**Figure 11**. Roll-Separating Force as a Function of Thickness for Four Different Sample Widths at a 0.3 Friction Coefficient for the B&W cold rolling mill

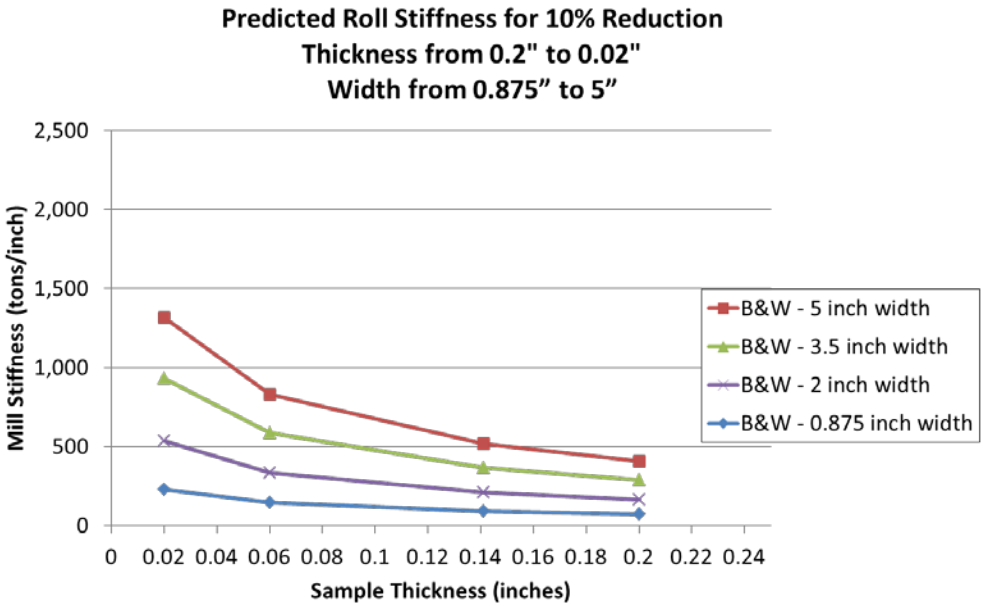


**Figure 12**. Mill Stiffness as a Function of Thickness for Four Different Sample Widths at a 0.3 Friction Coefficient

Another set of simulations was conducted for hot and cold rolling using B&W’s hot-rolling mill with a 16" diameter roll and their cold-rolling mill with a 3.75" diameter roll. Cold-rolling simulations were conducted with 10% reduction per pass and hot rolling with 15% reduction per pass. Initial sample dimensions were 4" in length, 4" in width, and 0.2" in thickness. Roll-separating force for both hot- and cold-rolling cases as a function of number of passes is plotted in Figure 13. Temperature was set to 700°C (1290°F) for the hot-rolling case with reheats between every two passes.

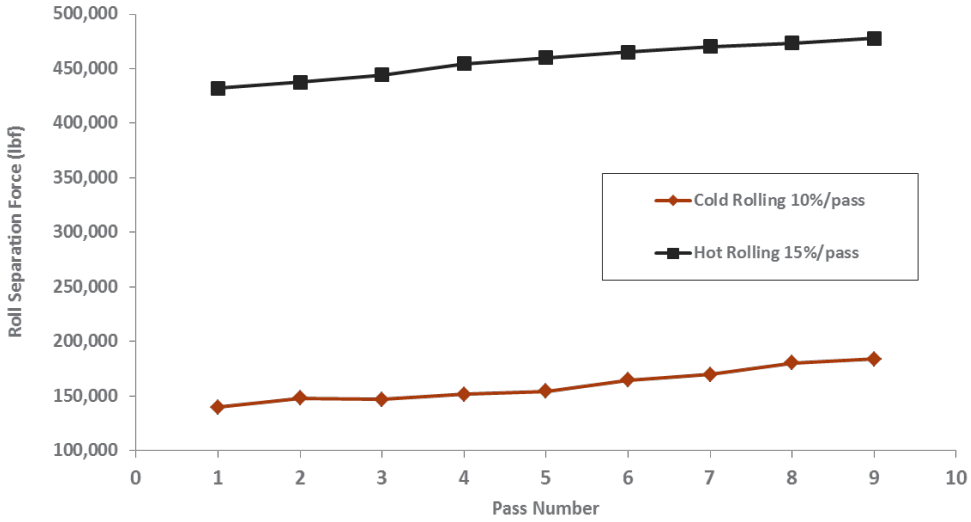


**Figure 13. Roll-separating force for both hot- and cold-rolling cases as a function of number of passes**

# 4.0 Surface Roughness Microstructure Modeling

## 4.1 Surface Roughness Observations

Figure 14 shows a 200× optical micrograph that reveals considerable thickness variation in zirconium layers on both sides of the foil. The top and bottom areas of this micrograph represent areas with high surface roughness at the interface between Zr and U-10Mo. This phenomenon is not desirable in fuel fabrication because thickness uniformity is an important aspect of the finished product.


**Figure 14**. Example of Typical Surface Roughness at the Interface between Zr and U-10Mo (Edwards et al. 2012)

A closer look at the micrograph in Figure 14 also reveals a disparity in the grain size of the U-10Mo. Grain sizes ranging from 1 to 4 orders of magnitude from one to another along the interface are observed. This variation in grain size is thought to be one major factor causing the surface roughness. A uniform grain size distribution may lead to a smoother and more uniform surface at the interface.

## 4.2 Microstructure Modeling

In order to investigate this surface roughness hypothesis, a microstructure-based FEM was developed to model the surface roughness of the U-10Mo/Zr interface. This approach uses randomly generated representative volume elements (RVEs) of the U-10Mo and zirconium layers, and uniform hexagonal shaped grains for the steel can; the model is depicted in Figure 15.

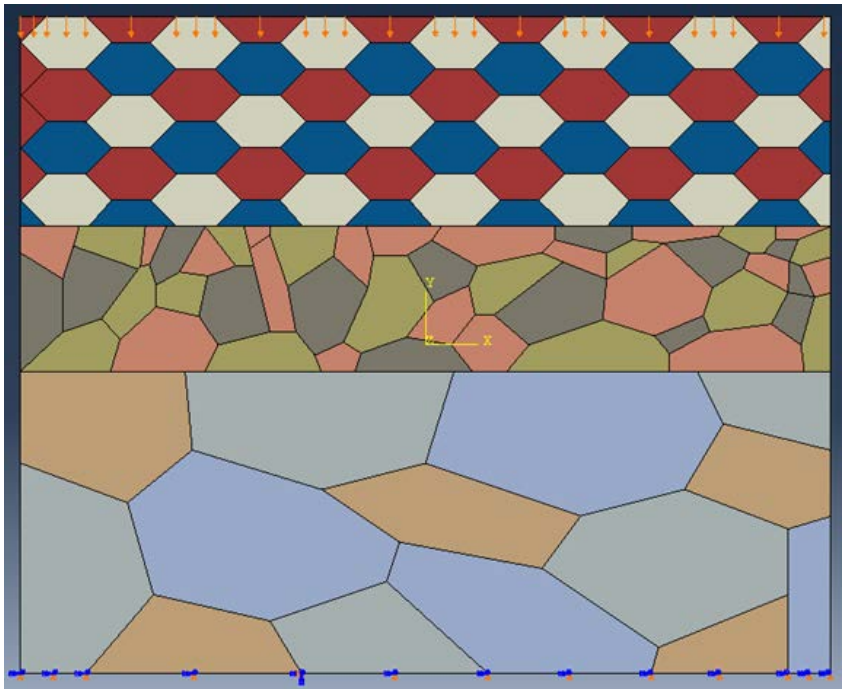

**Figure 15**. Representative Volume Element of the FEM-Based Microstructure Model Used for Surface Roughness Simulations. The layers are U-10Mo (bottom), Zr (middle) and the steel can (top).

The RVE is subjected to periodic boundary conditions at both sides and is not allowed to move vertically at the bottom, but is allowed to deform laterally. A displacement is imposed on the top side of the RVE to simulate a compression, such as that experienced during rolling. Each color in Figure 15 represents a group of grains with different orientation. Difference in orientation was taken into account in the model by different mechanical properties for each group of grains. This difference in mechanical properties is due to the difference in Mo concentration from one grain to another. Isotropy inside the grains was assumed for the current case.

Figure 16 represents a magnified Zr/U-10Mo interface before deformation on the left side, and after deformation on the right side. Surface roughness is observed, which is mainly due to the mismatch in strength between the U-10Mo grains and zirconium. This surface roughness attributed to the mismatch in strength between the two materials is also caused by the difference in Mo concentration and orientation

between U-10Mo grains present at the interface. A more uniform grain size of U-10Mo is expected to reduce this roughness and will be investigated further using this model. In addition, finer grains are more likely to behave better at the interface and reduce roughness. These assumptions are likely to be supported by modeling predictions from simulations currently ongoing.

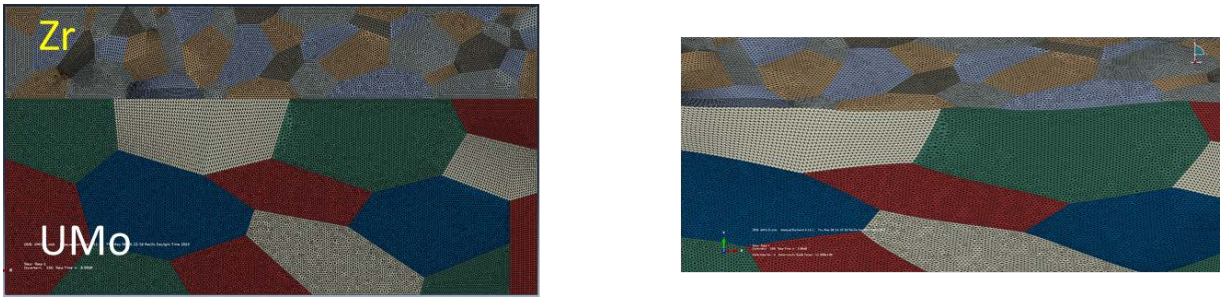


**Figure 16**. Magnified Interface between Zr and U-10Mo (left) Before Deformation and (right) After Deformation

# 5.0 Summary

The goal of the process modeling effort is to provide members of the FFC project that are rolling U-10Mo with the data needed to be sure they are rolling a high quality product in the most efficient manner possible. Therefore, the effort has focused on validation of the models with actual rolling data from PNNL and INL rolling mills. Through verification and validation, the model was used to determine forces at various rolling mills under many temperatures, reductions per pass and input/output thicknesses. As a result, B&W successfully rolled U-10Mo at approximately 600°C using 40% reduction of area rather than the small conservative reductions (typically less than 10%) previously used for U-10Mo. The model predicted that the rolling forces would be within the capability of the B&W mill.

Specific conclusions are summarized below:

- The previously developed FEM was further validated through comparison with hot- and cold-rolling data from experiments conducted at PNNL. This validated model was used to predict rolling forces at all FFC project rolling facilities.
- Friction coefficient values were back-calculated and established in the range of 0.3 to 0.5. A value of 0.3 was adopted for the simulations presented in this report and also for ongoing simulations.
- Parametric studies on the influence of roll diameter, temperature, and reduction on roll-separating force and mill stiffness were conducted, and results presented for the five rolling mills used within the FFC project. Dialogue between PNNL and B&W assured that 40% reduction per pass would be within the separation force capability of the production hot mill and was validated recently during B&W's initial U-10Mo hot-rolling campaign. Similar dialogue is underway for the cold rolling.
- Reduction rate was shown to be an important factor in obtaining uniform through-thickness strains. In fact, the smaller the reduction, the more likely only the coupon surface is worked and deformation of the coupon core is not achieved, which results in inhomogeneous deformation and potentially diverse final microstructure.

- A more detailed parametric study was conducted on the B&W rolling mills (both hot- and cold-rolling mills) and results on the effect of sample geometry (thickness and width) were presented in this report. The model predicts that the B&W rolling facilities will have the capacity to achieve reductions that produce uniformly deformed materials. The uniform through-thickness deformation will produce a more consistent quality product.
- A microstructure-based FEM was presented and initial results of the simulations of surface roughness at the Zr/U-10Mo interface were presented. Surface roughness was attributed to the mismatch in strength between the two materials and the difference in Mo concentration and orientation between the grains.
- Parametric studies are currently being conducted on grain size and carbide concentration and distribution to better understand the role of starting microstructure on the final product. Of particular interest is the impact of initial microstructure on surface roughness and thickness of the Zr diffusion barrier. Grain size, orientation and second-phase particles are likely to impact the uniformity of the deformation the in the U-10Mo.

# 6.0 References


Edwards DJ, RM Ermi, AL Schemer-Kohrn, NR Overman, CH Henager, Jr., D Burkes, and DJ Senor. 2012. "Characterization of U-Mo Foils for AFIP-7." PNNL-21990, Pacific Northwest National Laboratory, Richland, Washington.

Joshi VV, EA Nyberg, CA Lavender, D Paxton, H Garmestani, and DE Burkes. 2013. "Thermomechanical process optimization of U-10 wt% Mo – Part 1: high-temperature compressive properties and microstructure." *J. Nucl. Mater*, doi:10.1016/j.jnucmat.2013.10.065.

Lee DB, KH Kim, and CK Kim. 1997. "Thermal compatibility studies of unirradiated U–Mo alloys dispersed in aluminum." *J. Nucl. Mater*, 250(1):79–82.

Lenard LG, M Pietrzyk, and L Cser. 1999. "Mathematical and physical simulation of the properties of hot rolled product." Elsevier Science, Oxford, UK.

Meyer MK, GL Hofman, SL Hayes, CR Clark, TC Wiencek, JL Snelgrove, RV Strain, and K-H Kim. 2002. "Low-temperature irradiation behavior of uranium–molybdenum alloy dispersion fuel." *J. Nucl. Mater*, 304(2):221–236.

Ozaltun H, M-H Shen, and P Medvedev. 2011. "Assessment of residual stresses on U10Mo alloy based monolithic mini-plates during Hot Isostatic Pressing." *J. Nucl. Mater*, 419(1-3):76–84.

Park JM, KH Kim, CK Kim, MK Meyer, GL Hofman, and RV Strain. 2001. "The irradiation behavior of atomized U-Mo alloy fuels at high temperature." *J. Met. Mater. Int.*, 7(2):151–157.

Soulami A, C Lavender, D Paxton, and D Burkes. 2014. “Rolling Process Modeling Report: Finite-Element Prediction of Roll-Separating Force and Rolling Defects.” PNNL-23313, Pacific Northwest National Laboratory, Richland, Washington.

Snelgrove JL, GL Hofman, and MK Meyer. 1997. “Development of very high density low-enriched Uranium fuels.” *J. Nucl. Eng. Des.*, 178:119-126.

Sun W, K Tieu, H Li, Z Jiang, G Wang, and Z Liu. 2005. “Friction in the roll bite under various hot rolling conditions.” Presented at the 3rd symposium on advanced structural steel and new rolling technologies, Northeastern University, Shenyang, China.

# Distribution

**No. of Copies**

1 Department of Energy
National Nuclear Security Administration
Global Threat Reduction Initiative
1000 Independence Ave.
Washington, D.C. 20002-USA
Mr. Christopher Landers
Mr. Bryan Reed (PDF)

1 Idaho National Laboratory
P.O. Box 1625
Idaho Falls, ID 83415
Mr. Kenneth Rosenberg
Dr. Barry Rabin (PDF)

2 Argonne National Laboratory
9700 S. Cass Ave.
Argonne, IL 60439
Dr. Erik Wilson

**No. of Copies**

4 **Local Distribution**
Pacific Northwest National Laboratory

| | |
|---|---|
| D.E. Burkes | K8-34 |
| D.M. Paxton | K2-03 |
| C.A. Lavender | K2-03 |
| A. Soulami | K2-03 |

Pacific Northwest
NATIONAL LABORATORY

*Proudly Operated by* **Battelle** *Since 1965*

U.S. DEPARTMENT OF
ENERGY

902 Battelle Boulevard
P.O. Box 999
Richland, WA 99352
**1-888-375-PNNL** (7665)

***www.pnnl.gov***